

Exploring DNA Dynamics: A Mathematical Model of M.Tuberculosis and M.Bovis BCG1 Interactions

Gunasekaran.M¹, Alamelu.K^{2*}

¹*PG Department of Mathematics, Sri Subramaniyaswamy Government Arts College, Tiruttani - 631 209, India.*

²*Department of Mathematics, Nazareth College of Arts and Science, Avadi, Chennai–600062, India.*

²*Research Scholar, PG Department of Mathematics, Sri Subramaniyaswamy Government Arts College, Tiruttani - 631209, India., *alameluiyappan@gmail.com.*

Abstract

This study presents an ordinary differential equation (ODE) model designed to simulate the interaction between M.tuberculosis and M.bovis BCG1, with measurements in DNA/fg/cell. The model can be solved using either the Runge-Kutta fourth-order method or Euler's method, both of which can be implemented using Python. This framework provides a comprehensive tool for analysing the dynamic relationship between these two microorganisms. The model allows for the examination of how various factors, including different parameters, initial conditions, boundary conditions and time steps, influence the interaction between M.tuberculosis and M.bovis BCG1. Additionally, the model offers insights into the effects of various numerical techniques on the system's behaviour. By adjusting these conditions and methods, the model can be used to explore the complex interplay between these organisms under different scenarios, providing a deeper understanding of their interaction dynamics. This ODE-based approach serves as a versatile tool for researchers aiming to investigate and predict the outcomes of specific changes in the interaction between M. tuberculosis and M. bovis BCG1, thereby contributing to advancements in tuberculosis research and vaccine development.

Keywords: M.Tuberculosis (DNA/fg/cell), M. bovis BCG1 (DNA/fg/cell), ODE model,Eulers model,Rk4 method.

1. Introduction

Mathematical models are essential for understanding and controlling infectious diseases. This enables the simulation of disease transmission, assessment of intervention impacts, and prediction of outbreaks. By integrating pathogen characteristics, host behaviour, optimal harvesting and environmental factors [7, 8, 9], these models offer crucial insights into the spread of infections and inform public health strategies. [6,17]. The importance of mathematical modelling has been particularly evident during the COVID-19 pandemic. A study in Nature (2020) demonstrated how models were used to predict virus transmission, evaluate social distancing measures, and forecast healthcare system burdens, thereby guiding policy decisions and resource allocation.[5,12,16]. Furthermore, mathematical models are increasingly applied to study antimicrobial resistance (AMR). A 2021 study in The Lancet Infectious Diseases showcased how models can estimate the future burden of AMR, evaluate treatment strategies, and aid in developing new therapies [18].This highlights the growing role of mathematical modelling in addressing complex challenges in infectious disease management.

Numerous studies have shown that deciphering the 3-dimensional (3D) double helical structure of DNA is crucial for understanding the specificity of transcription factor (TF) binding and its effects on gene

expression [1,20]. DNA shape and flexibility are key factors influencing DNA-TF recognition, with each factor affecting binding in slightly different ways depending on the context [2,3,13]. Many biological processes rely on DNA deformation, which is influenced by the DNA's structure, mechanical properties, and surface topography [10,19]. Therefore, the intrinsic structural features of DNA—such as its deformability, duplex stability, curvature, groove shape, and topography—provide more accurate indicators of TF-binding site specificity than merely the nucleotide sequence [4]. DNA bendability or nucleosome positioning preference (NPP) models [14], as well as DNA I sensitivity models [16], have been developed using trinucleotide models to assess the adaptability of DNA sequences [15]. Over the past 20 years, research has highlighted the role of intrinsic DNA curvature in important biological processes such as transcription, recombination, replication and chromatin organization. Bent DNA segments are often found near functionally critical sites such as replication origins and promoters. Several models, including the BMHT model derived from gel mobility assays and the CS model based on crystal structure data have been proposed to explain DNA curvature. The BMHT model was constructed using large datasets and various methods, considering 16 roll and tilt angles. However, it tends to favor AA/TT steps while overlooking motifs like GGGCCC and rare helical phasing sequences [11]. After Z-score normalization for each TF, global bendability properties and DNA shape characteristics for 51 TFs in the extended dataset were visualized using a heatmap.

2. Mathematical Model for M.Tuberculosis (DNA/fg/cell) and M.Bovis BCG1 (DNA/fg/cell)

The variable M.T. (DNA) represents the density of the prey population, while M.BCG1 (DNA) corresponds to the predator population density, with t indicating time. The prey's growth characteristics are defined by α_5 and β_5 , where α_5 signifies the maximum growth rate per individual, and β_5 reflects the effect of predators on the prey's growth rate. Similarly, the predator's growth characteristics are described by γ_5 and δ_5 with γ_5 representing the maximum growth rate per individual and δ_5 indicates the influence on the prey's growth. The initial conditions are given as $\alpha_5 = 1$ (representing the mortality rate due to predation), $\beta_5 = 1$, $\delta_5 = 1$, $\gamma_5 = 2$, with $x_0 = 6.90$, $y_0 = 6.73$, $t = 30$ days and $t_{max} = 23.10$.

$$\frac{d(M.T.(DNA))}{dt} = \alpha_5(M.T.(DNA)) - \beta_5(M.T.(DNA))(M.BCG1(DNA)) \quad \dots (1)$$

$$\frac{d(M.BCG1(DNA))}{dt} = \delta_5 \left(M.T.(DNA)(M.BCG1(DNA)) - \gamma_5(M.BCG1(DNA)) \right) \quad \dots (2)$$

This equation (1) and (2) gives us two equilibrium points $(0,0)$ and $\left(\frac{\delta_5}{\gamma_5}, \frac{\alpha_5}{\beta_5}\right)$. To determine the stability of these equilibrium points, we can use the Jacobian matrix. Evaluating the Jacobian at each equilibrium point, we get

$$J(M.T.(DNA), M.BCG1(DNA)) = \begin{pmatrix} \alpha_5 + \beta_5(M.BCG1(DNA)) & \beta_5(M.T.(DNA)) \\ -\gamma_5(M.BCG1(DNA)) & \delta_5 - \gamma_5(M.T.(DNA)) \end{pmatrix}$$

Evaluating the jacobian at each equilibrium point, we get

$$\begin{pmatrix} \alpha_5 & 0 \\ 0 & \delta_5 \end{pmatrix} J\left(\frac{\delta_5}{\gamma_5}, \frac{\alpha_5}{\beta_5}\right) = \begin{pmatrix} \alpha_5 & \beta_5 \left(\frac{\alpha_5}{\beta_5}\right) \\ -\gamma_5 \left(\frac{\delta_5}{\gamma_5}\right) & \delta_5 \end{pmatrix}$$

The eigen values of $J(0,0)$ are $\lambda_1 = \alpha_5$ and $\lambda_2 = \delta_5$ so stability of $(0,0)$ depends on the signs of α_5 and δ_5 . If $\alpha_5 < 0$ and $\delta_5 < 0$, then $(0,0)$ is a stable node. If $\alpha_5 < 0$ and $\delta_5 > 0$, then $(0,0)$ is an unstable node. If $\alpha_5 \delta_5 < 0$, then $(0,0)$ is a saddle point. If $\delta_5 > 0$, then $(0,0)$ is an unstable node.

The eigenvalues of $J\left(\frac{\delta_5}{\gamma_5}, \frac{\alpha_5}{\beta_5}\right)$ are $\lambda_1 = \alpha_5 + \frac{\beta_5}{\gamma_5} \delta_5$ and $\lambda_2 = \delta_5 - \frac{\gamma_5}{\beta_5} \alpha_5$, so the stability of $\left(\frac{\delta_5}{\gamma_5}, \frac{\alpha_5}{\beta_5}\right)$ depends on the signs of $\alpha_5 + \frac{\beta_5}{\gamma_5} \delta_5$ and $\delta_5 - \frac{\gamma_5}{\beta_5} \alpha_5$. Both eigen values have the same sign, then $\left(\frac{\delta_5}{\gamma_5}, \frac{\alpha_5}{\beta_5}\right)$ is a

stable node or a staple spiral, depending on whether the eigen values are negative or positive. If the eigenvalues have opposite signs, then $\left(\frac{\delta_5}{\gamma_5}, \frac{\alpha_5}{\beta_5}\right)$ is a saddle point. If one eigen value is zero, then we need to use higher-order terms to determine the stability.

3. ODE Model for M.Tuberculosis (DNA/fg/cell) and M.Bovis BCG1 (DNA/fg/cell)

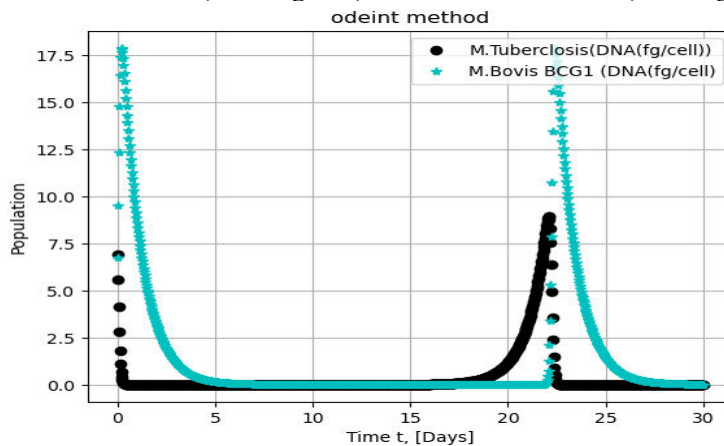


Figure: 1 Interaction of ode model Tuberculosis (DNA/fg/cell) and M.Bovis BCG1 (DNA/fg/cell)

Time (t-days)	M.Tuberculosis(DNA(fg/cell))	M.Bovis BCG1 DNA(fg/cell)
30	6.90000000e+00	6.73000000e+00
30	5.57611049e+00	9.51057868e+00
30	4.13596580e+00	1.23536438e+01
30	5.60320541e-06	1.01875376e-02
30	5.77228188e-06	9.88615683e-03
30	5.94651325e-06	9.59369204e-03

Table: 1 Interaction of ode model Tuberculosis (DNA/fg/cell) and M.Bovis BCG1 (DNA/fg/cell)

The **figure 1** focuses on two bacterial species, *Mycobacterium tuberculosis* and *Mycobacterium bovis* BCG1, analyzing the amount of DNA (measured in femtograms per cell, fg/cell) present at different intervals of 30 days each. Initially, after 30 days, the DNA concentration was approximately 6.9 fg/cell for *M. tuberculosis* and 6.73 fg/cell for *M. bovis* BCG1. At the next 30-day interval, the *M. tuberculosis* DNA decreased to about 5.58 fg/cell, while *M. bovis* BCG1 increased to 9.51 fg/cell. By the third 30-day mark, the DNA concentration of *M. tuberculosis* further declined to approximately 4.14 fg/cell, with *M. bovis* BCG1 rising to 12.35 fg/cell. In the fourth interval, the *M. tuberculosis* DNA was recorded at around 0.00000560320541 fg/cell, and *M. bovis* BCG1 at 0.0101875376 fg/cell. By the fifth interval, *M. tuberculosis* DNA slightly increased to 0.00000577228188 fg/cell, with a slight decrease in *M. bovis* BCG1 DNA to 0.00988615683 fg/cell. Finally, at the sixth interval, *M. tuberculosis* DNA increased marginally to 0.00000594651325 fg/cell, while *M. bovis* BCG1 DNA decreased to 0.00959369204 fg/cell. A phase plane graph comparing the DNA concentrations of these two bacteria shows an inverse relationship between the two. The x-axis represents *M. tuberculosis* DNA per cell, ranging from 0 to 6 fg/cell, while the y-axis represents *M. bovis* BCG1 DNA per cell, ranging from 0 to 12 fg/cell. The blue curve illustrates that as *M. tuberculosis* DNA increases, *M. bovis* BCG1 DNA decreases significantly, suggesting a sharp inverse correlation between these variables.

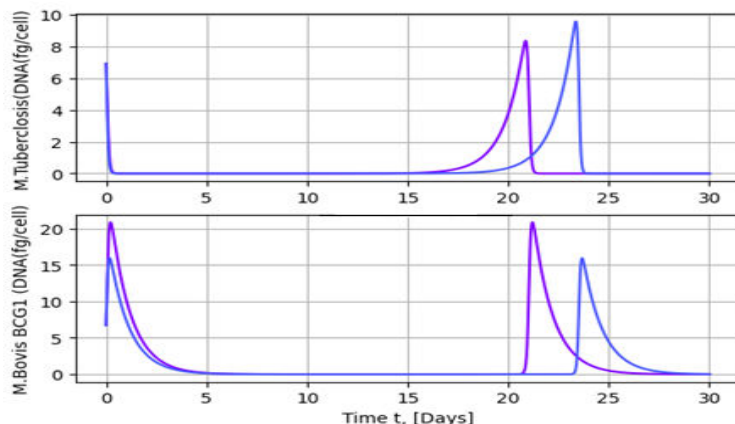


Figure: 2 Interaction of random model Tuberculosis (DNA/fg/cell) and M. Bovis BCG Glaxo (DNA/fg/cell)

TIME (t-days)	M.Tuberculosis(DNA(fg/cell))	M.Bovis BCG1 DNA(fg/cell)
30	6.90000000e+00	6.73000000e+00
30	5.85040050e+00	9.59047932e+00
30	4.61052088e+00	1.27482452e+01
30	6.12506452e-05	3.55048602e-03
30	6.31125972e-05	3.44546273e-0320
30	6.50313120e-05	3.34354639e-03
30	6.90000000e+00	6.73000000e+00
30	5.31611914e+00	9.43393500e+00
30	3.71861496e+00	1.19990430e+01
30	4.80297861e-07	3.17455891e-02
30	4.94382499e-07	3.08064410e-02
30	5.08897133e-07	2.98950762e-02

Table: 2 interaction of Random model Tuberculosis (DNA/fg/cell) and M. Bovis BCG Glaxo (DNA/fg/cell)

The **figure 2** displays the DNA concentration (measured in femtograms per cell) of two bacterial species, *Mycobacterium tuberculosis* and *Mycobacterium bovis BCG1*, over a series of time intervals, each spanning 30 days. The x-axis represents the concentration of *M. tuberculosis* DNA per cell, ranging from 0 to 6 fg/cell, while the y-axis shows the concentration of *M. bovis BCG1* DNA per cell, ranging from 0 to 12 fg/cell. The graph reveals an inverse relationship between the two variables, as depicted by the blue curve. Specifically, as the concentration of *M. tuberculosis* DNA increases, the concentration of *M. bovis BCG1* DNA decreases sharply.

Over the 30-day intervals, the data reveals the following trends: Initially, the DNA concentration of *M. tuberculosis* is approximately 6.9 fg/cell, and that of *M. bovis BCG1* is about 6.73 fg/cell. By the second interval, *M. tuberculosis* DNA decreases to 5.85 fg/cell, while *M. bovis BCG1* DNA rises to 9.59 fg/cell.

At the third interval, *M. tuberculosis* DNA further drops to 4.61 fg/cell, and *M. bovis BCG1* DNA increases to 12.75 fg/cell. By the fourth interval, *M. tuberculosis* DNA is nearly 0.0000612506452 fg/cell, with *M. bovis BCG1* DNA at 0.00355048602 fg/cell. This trend continues with slight increases in *M. tuberculosis* DNA and corresponding decreases in *M. bovis BCG1* DNA through the fifth and sixth intervals.

After the sixth interval, the pattern repeats: at the seventh interval, *M. tuberculosis* DNA is again around 6.9 fg/cell, and *M. bovis BCG1* DNA is 6.73 fg/cell. By the eighth interval, *M. tuberculosis* DNA decreases to 5.32 fg/cell, and *M. bovis BCG1* DNA rises to 9.43 fg/cell. The ninth interval shows *M. tuberculosis* DNA at 3.72 fg/cell and *M. bovis BCG1* DNA at 12 fg/cell. Finally, at the tenth interval,

M.tuberculosis DNA concentration drops to approximately 0.000000480297861 fg/cell, while M.bovis BCG1 DNA increases to 0.0317455891 fg/cell. This trend continues into the eleventh and twelfth intervals, with M. tuberculosis DNA at 0.000000494382499 fg/cell and 0.000000508897133 fg/cell, and M. bovis BCG1 DNA at 0.030806441 fg/cell and 0.0298950762 fg/cell, respectively.

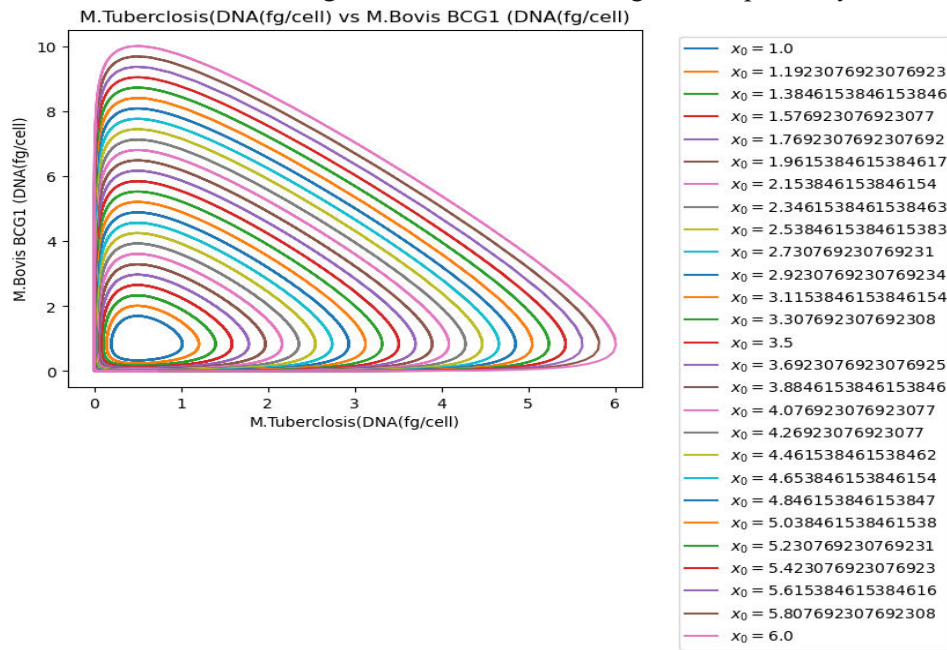


Figure: 3 Interaction of M. Tuberculosis (DNA/fg/cell) VsM.Bovis BCG1 (DNA/fg/cell)

In **figure 3**, the phase plane graph illustrates the DNA concentrations (in femtograms per cell) of two bacterial species, *Mycobacterium tuberculosis* and *Mycobacterium bovis* BCG1. The x-axis denotes the amount of *M.tuberculosis* DNA per cell, ranging from 0 to 6 fg/cell, while the y-axis shows the amount of *M.bovis* BCG1 DNA per cell, spanning from 0 to 12 fg/cell. The graph features several curves, each corresponding to different initial conditions that vary from 1.0 to 6.0. These curves depict how the DNA concentrations of the two bacteria evolve over time based on each initial condition.

3.1. Tuberculosis (DNA/fg/cell) and M.Bovis BCG1 (DNA/fg/cell) using Euler's Model

Starting with an initial value, first-order numerical methods, such as Euler's method, can be employed to solve ordinary differential equations (ODEs). This method estimates the value of $y(x+h)$ by constructing a tangent line at point xxx , where the slope is given by $y'(x)$. Euler's method approximates the solution by using this tangent lines—represented as a sequence of short line segments—across intervals of width h . To enhance the accuracy of the approximation, smaller step sizes can be utilized. For a given position b , the generic formula $y(b)$, where h represents the step size, provides the functional value and $Y(b)$, with h indicates the time step.

$$Y(b) = y(a) + h * \sum_{i=1}^n f(X_{i-1}, y_{i-1}) \text{ where } X_i = X_{i-1} + h, y_i = y_{i-1} + h * f(X_{i-1}, y_{i-1})$$

Here, $f(x, y)$ represents the derivative of y with respect to x . Euler's method is a simple and effective way to solve ODEs numerically, despite having a few flaws.

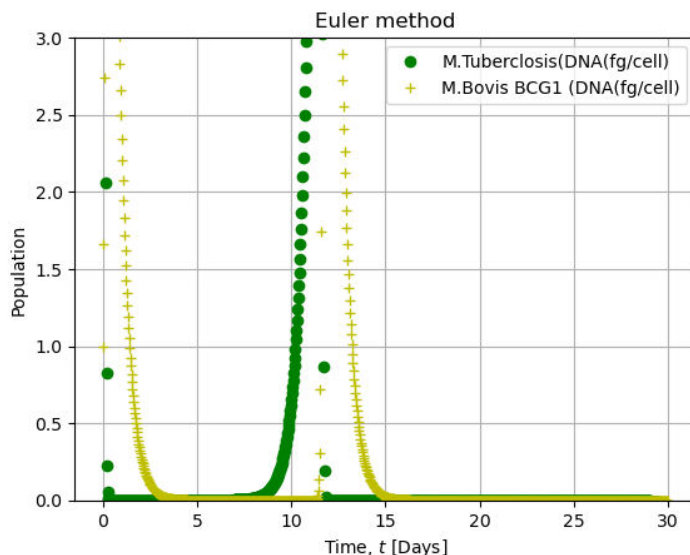


Figure: 4 Interaction of Eulers model Tuberculosis (DNA/fg/cell) and M.Bovis BCG1 (DNA/fg/cell)

TIME (t-days)	M.Tuberculosis(DNA(fg/cell)	M.Bovis BCG1 DNA(fg/cell)
30	6.00000000e+00	1.00000000e+00
30	5.92792793e+00	1.66066066e+00
30	5.57446221e+00	2.74341698e+00
30	-3.31237712e-02	9.78616754e-16
30	-3.51131869e-02	9.15947222e-16
30	-3.72220870e-02	8.57072095e-16

Table: 4 Interaction of Eulers model Tuberculosis (DNA/fg/cell) and M.Bovis BCG1 (DNA/fg/cell)

The **figure 4** shows the results of a population study using the Euler method, comparing the growth of two different bacterial strains: *Mycobacterium tuberculosis* (*M. tuberculosis*) and *Mycobacterium bovis* BCG1 (*M. bovis* BCG1). The x-axis represents time in days, and the y-axis represents population in DNA (fg/cell). Both strains exhibit a pattern of rapid growth followed by a sharp decline, with two distinct peaks occurring around days 5 and 15. *M. tuberculosis* (indicated by green circles) generally has a higher peak population than *M. bovis* BCG1 (indicated by yellow crosses) in both instances. This suggests that *M. tuberculosis* has a more robust growth rate or higher population density compared to *M. bovis* BCG1 under the conditions modelled. The sharp rise and fall in population indicate that the growth phase of these bacterial strains is quick, and they may undergo a rapid depletion of resources or reach a stage where their population can no longer be sustained, leading to a rapid decline. The graph also illustrates that the growth cycles of these two strains are similar in timing but differ in magnitude.

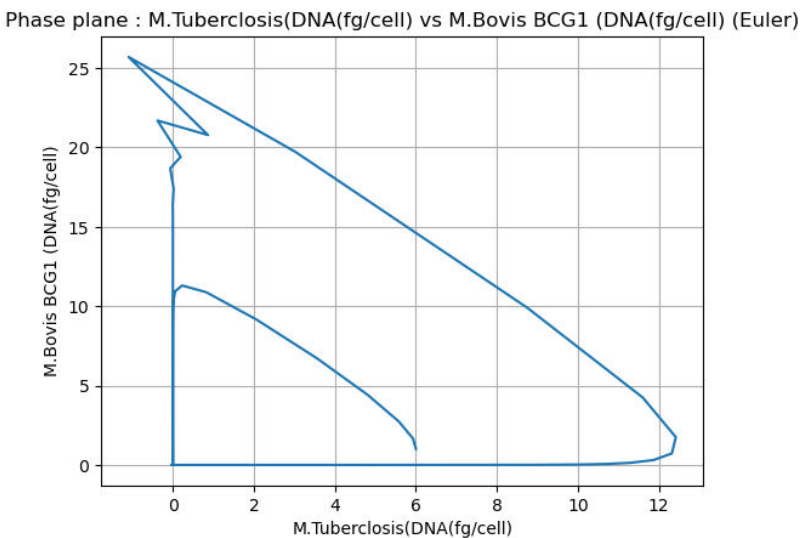


Figure: 5 Phase plane of Tuberculosis (DNA/fg/cell) and M.Bovis BCG1 (DNA/fg/cell)

The figure 5 presented focuses on the DNA concentrations of *Mycobacterium tuberculosis* and *Mycobacterium bovis BCG1* measured in femtograms per cell (fg/cell) over a 30-day period. At the first time point, the DNA concentration is approximately 6 fg/cell for *M. tuberculosis* and 1 fg/cell for *M. bovis BCG1*. By the second time point, *M. tuberculosis* DNA slightly decreases to about 5.93 fg/cell, while *M. bovis BCG1* DNA increases to around 1.66 fg/cell. At the third time point, *M. tuberculosis* DNA further decreases to 5.57 fg/cell, with *M. bovis BCG1* DNA rising to approximately 2.74 fg/cell. However, at the fourth time point, the DNA concentration for both bacteria drops significantly, with *M. tuberculosis* showing about -0.033 fg/cell and *M. bovis BCG1* almost negligible at 0.000000000000000978616754 fg/cell. The trend continues similarly at the fifth and sixth time points, where the DNA concentrations for *M. tuberculosis* are around -0.035 fg/cell and -0.037 fg/cell, and for *M. bovis BCG1*, they are approximately 0.000000000000000915947222 fg/cell and 0.000000000000000857072095 fg/cell, respectively.

Additionally, a phase plane graph is provided, which compares the DNA concentrations of the two bacterial strains. The x-axis of the graph represents the DNA concentration of *M. tuberculosis* per cell, ranging from 0 to 6 fg/cell, while the y-axis represents the DNA concentration of *M. bovis BCG1*, ranging from 0 to 12 fg/cell. The graph includes several curves, each corresponding to a different initial condition ranging from 1.0 to 6.0. These curves illustrate how the DNA concentrations of *M. tuberculosis* and *M. bovis BCG1* evolve over time based on their respective initial conditions.

3.2. Runge-kutta Model for Tuberculosis (DNA/fg/cell) and M.Bovis BCG1(DNA/fg/cell)

A numerical method for resolving ordinary differential equations of the form $dy/dx = f(x, y)$, $y(x(0)) = y(0)$ is the fourth-order Runge-Kutta method. Comparing this improvement to the first-order Euler's approach, it yields greater precision with fewer computations. One of the most popular Runge-Kutta techniques for solving differential equations is the fourth-order method. Despite requiring more computing power, the RK4 technique is more accurate than Euler's method. Because of the technique's precision and versatility, scientific computing uses it extensively. [12].

Assuming h to be the time step, we can write: $y_{i+1} = y_i + \frac{1}{6}(k_1 + 2k_2 + 2k_3 + k_4)$

$$\text{Where } K_1 = hf(X_i, y_i)$$

$$K_2 = hf\left(X_i + \frac{h}{2}, y_i + \frac{K_1}{2}\right)$$

$$K_3 = hf\left(X_i + \frac{h}{2}, y_i + \frac{K_2}{2}\right)$$

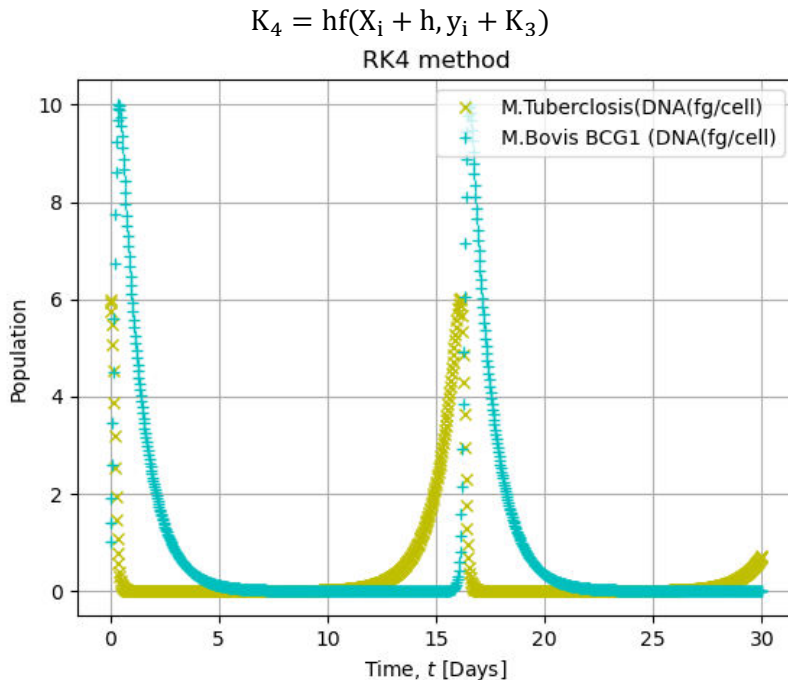


Figure: 6 Interaction of RK4 model Tuberculosis (DNA/fg/cell) and M.Bovis BCG1 (DNA/fg/cell)

TIME (t-days)	M.Tuberculosis(DNA(fg/cell))	M.Bovis BCG1 DNA(fg/cell)
30	6.00000000e+00	1.00000000e+00
30	5.92462481e+00	1.38882460e+00
30	5.75506592e+00	1.91492644e+00
30	6.81799446e-01	6.37242313e-05
30	7.02582806e-01	6.44638612e-05
30	7.23999686e-01	6.52947635e-05

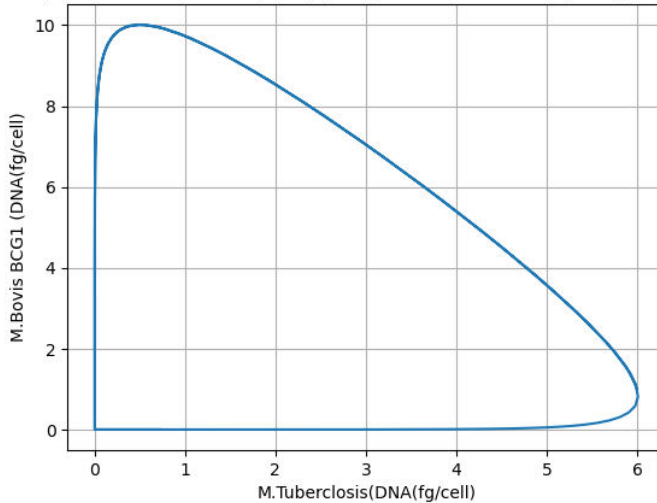
Table: 6 interaction of RK4 model Tuberculosis (DNA/fg/cell) and M.Bovis BCG1 (DNA/fg/cell)

The figure 6 depicts the population of two types of bacteria, **Mycobacterium tuberculosis** and **Mycobacterium bovis BCG1**, over time. The time is measured in days. Here's a general interpretation of the graph: The x-axis represents time in days, ranging from 0 to 30. The y-axis represents the population of cells, ranging from 0 to 3.0. Two types of cells are represented: M. Tuberculosis (green dots) and M. Bovis BCG1 (yellow plus signs). Both cell populations increase until around day 10; M. Tuberculosis peaks at a higher population than M. Bovis BCG1. After peaking, both cell populations decline sharply; by day 20, they have nearly reached zero.

Mycobacterium tuberculosis and Mycobacterium bovis BCG1. The values represent the amount of DNA from each bacterium (in femtograms per cell, or fg/cell) at different time points (30 days). Here's a breakdown of the data. At the first time point (30 days), there are approximately 6 fg/cell of M. tuberculosis DNA and 1 fg/cell of M. bovis BCG1 DNA. At the second time point (also 30 days), there are approximately 5.92 fg/cell of M. tuberculosis DNA and 1.39 fg/cell of M. bovis BCG1 DNA. At the third time point (again 30 days), there are approximately 5.76 fg/cell of M. tuberculosis DNA and 1.91 fg/cell of M. bovis BCG1 DNA. At the fourth time point (still 30 days), there are approximately 0.682 fg/cell of M. tuberculosis DNA and 0.0000637242313 fg/cell of M. bovis BCG1 DNA. At the fifth time point (once more 30 days), there are approximately 0.703 fg/cell of M. tuberculosis DNA and 0.0000644638612

fg/cell of *M. bovis* BCG1 DNA. At the sixth time point (yet again 30 days), there are approximately 0.724 fg/cell of *M. tuberculosis* DNA and 0.0000652947635 fg/cell of *M. bovis* BCG1 DNA.

Phase plane : M.Tuberculosis(DNA(fg/cell)) vs M.Bovis BCG1 (DNA(fg/cell)) (RK4)

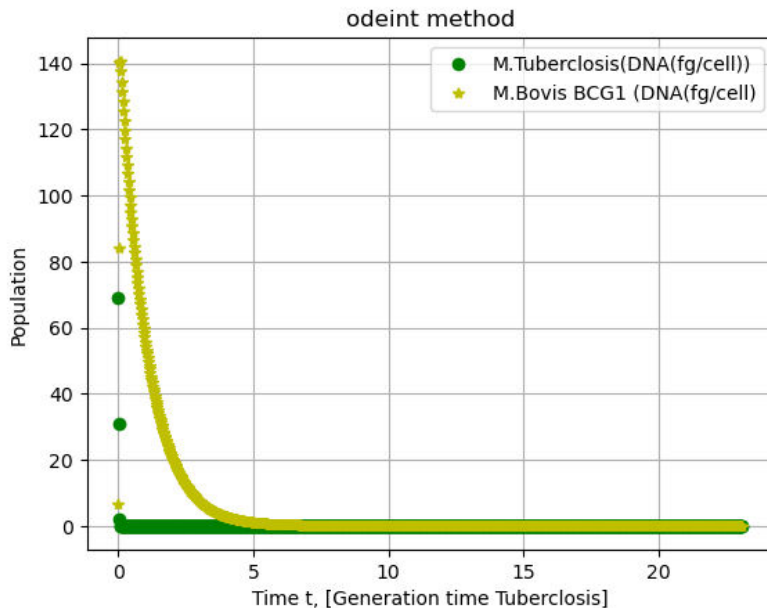
**Figure: 7 Interaction of RK4 model Tuberculosis (DNA/fg/cell) and M.Bovis BCG1 (DNA/fg/cell)**

In figure 7, a phase plane graph that compares the DNA concentration (in femtograms per cell) of two types of bacteria, **Mycobacterium tuberculosis** and **Mycobacterium bovis BCG1**. Here's a general interpretation of the graph:

The x-axis represents the quantity of *M. tuberculosis* DNA per cell, ranging from 0 to 6. The y-axis represents the quantity of *M. bovis* BCG1 DNA per cell, ranging from 0 to 12. The graph contains multiple curves, each representing a different initial condition ranging from 1.0 to 6.0. Each curve shows how the DNA concentration of the two bacteria changes over time for a given initial condition.

Generation time:

The tubercle bacillus is characterized by several unique features, including its intricate cell envelope, slow growth rate, ability to enter a dormant state, intracellular pathogenicity and genetic uniformity. When it comes to its generation time, *Mycobacterium tuberculosis* typically takes around 24 hours to divide, whether in infected animals or when cultured in synthetic media.

**Figure: 8 Interaction of ode model Tuberculosis (RNA/fg/cell) and M.Bovis BCG1 (RNA/fg/cell)**

Generation Time (t-days)	Tuberculosis(DNA(fg/cell)	M.Bovis DNA(fg/cell)	BCG1
23.10h	6.90000000e+01	6.73000000e+00	
23.10h	3.10451230e+01	8.43697226e+01	
23.10h	1.87044960e+00	1.40419230e+02	
23.10h	5.66824531e-04	1.47712989e-08	
23.10h	5.80085283e-04	1.44339444e-08	
23.10h	5.93656140e-04	1.41043082e-08	

Table: 8 Interaction of ode model Tuberculosis (DNA/fg/cell) and M.Bovis BCG1 (DNA/fg/cell)

In **figure 8**, The data obtained seems to pertain to a scientific study comparing two bacterial strains, *Mycobacterium tuberculosis* and *Mycobacterium bovis* BCG1. The measurements reflect the DNA concentration of each bacterium in femtograms per cell (fg/cell) at specific intervals of 23.10 hours.

At the first interval, the DNA concentration for *M. tuberculosis* is about 69 fg/cell, while for *M. bovis* BCG1, it is around 6.73 fg/cell. By the second interval, the DNA amount in *M. tuberculosis* decreases to approximately 31.045 fg/cell, whereas *M. bovis* BCG1 sees a significant increase to 84.37 fg/cell. In the third interval, *M. tuberculosis* DNA drops further to 1.87 fg/cell, while *M. bovis* BCG1 DNA spikes to about 140.42 fg/cell. The fourth interval shows a dramatic reduction in DNA levels, with *M. tuberculosis* at roughly 0.000566824531 fg/cell and *M. bovis* BCG1 at 0.000000000147712989 fg/cell. This trend continues in the fifth and sixth intervals, where the DNA concentration for *M. tuberculosis* remains around 0.000580085283 fg/cell and 0.00059365614 fg/cell, and for *M. bovis* BCG1, it stays near 0.000000000144339444 fg/cell and 0.0000000000141043082 fg/cell, respectively.

The accompanying graph tracks the population dynamics of *Mycobacterium tuberculosis* and *Mycobacterium bovis* BCG1 over time, with the x-axis representing time based on the generation time of *M. tuberculosis*, ranging from 0 to 20, and the y-axis showing the bacterial population. The green circles depict the *M. tuberculosis* population, which initially surges, reaching a peak close to 140 before rapidly declining and levelling off just above zero. Conversely, the yellow stars represent the *M. bovis* BCG1 population, which remains largely stable with minimal fluctuation, consistently staying near zero throughout the observed period.

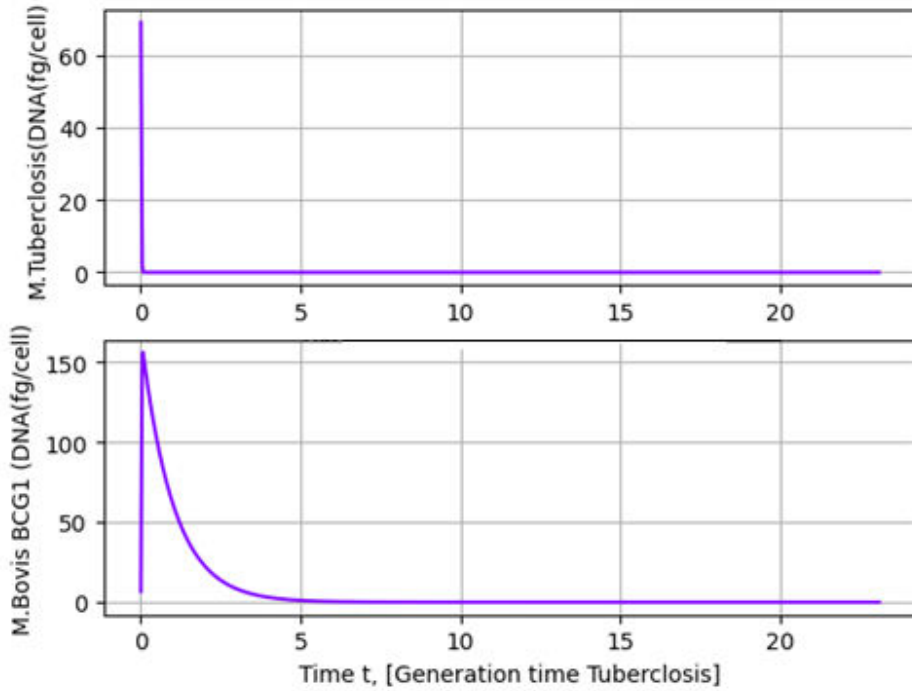


Figure: 9 Interaction of ODE model Tuberculosis (DNA/fg/cell) and M.Bovis BCG1 (DNA/fg/cell)

Generation Time (t-days)	M.Tuberculosis(DNA(fg/cell))	M.Bovis BCG1 DNA(fg/cell)
23.10h	6.9000000e+01	6.7300000e+00
23.10h	3.30820777e+01	8.85946961e+01
23.10h	2.11865168e+00	1.54970030e+02
23.10h	-1.16794382e-04	1.63704474e-08
23.10h	-1.19527363e-04	1.59955466e-08
23.10h	-1.22324109e-04	1.56293192e-08

Table : 9 interaction of Eulers model Tuberculosis (DNA/fg/cell) and M.Bovis BCG1 (DNA/fg/cell)

In figure 9, two line graphs that plot the concentration of DNA from two types of bacteria, **Mycobacterium tuberculosis** and **Mycobacterium bovis BCG1**, over time. Here's a breakdown of the graphs. The x-axis represents time in terms of the generation time of tuberculosis, ranging from 0 to 20. The first graph (top) shows the concentration of *M. tuberculosis* DNA (in femtograms per cell) on the y-axis, which ranges from 0 to 60. The concentration sharply decreases at the beginning and then stabilizes close to zero. The second graph (bottom) shows the concentration of *M. bovis BCG1* DNA (in femtograms per cell) on the y-axis, which ranges from 0 to 150. Similar to the first graph, the concentration rapidly decreases and stabilizes near zero.

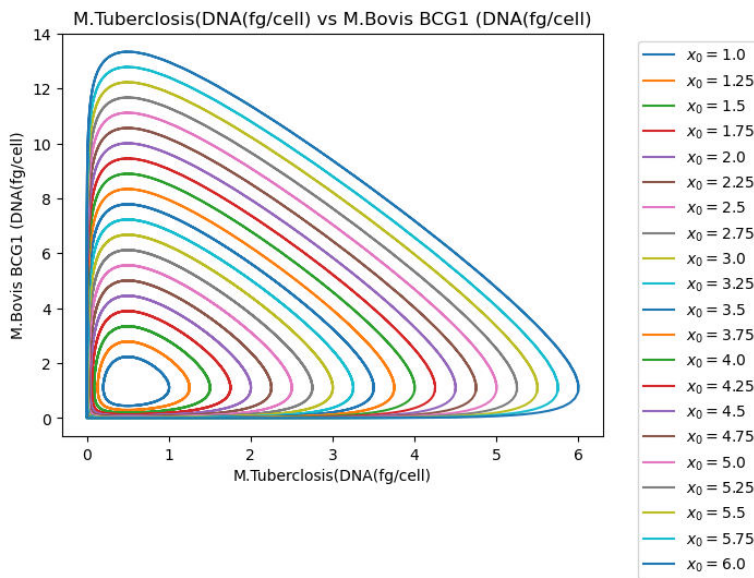


Figure: 10 Interaction of Eulers model Tuberculosis (DNA/fg/cell) and M.Bovis BCG1 (DNA/fg/cell)

The **figure 10** shows a scientific experiment involving two types of bacteria: *Mycobacterium tuberculosis* and *Mycobacterium bovis* BCG1. The values represent the amount of DNA from each bacterium (in femtograms per cell, or fg/cell) at different time points (23.10 hours). Here's a breakdown of the data. At the first time point (23.10 hours), there are approximately 69 fg/cell of *M. tuberculosis* DNA and 6.73 fg/cell of *M. bovis* BCG1 DNA.

At the second time point (also 23.10 hours), there are approximately 33.08 fg/cell of *M. tuberculosis* DNA and 88.59 fg/cell of *M. bovis* BCG1 DNA. At the third time point (again 23.10 hours), there are approximately 2.12 fg/cell of *M. tuberculosis* DNA and 154.97 fg/cell of *M. bovis* BCG1 DNA. At the fourth time point (still 23.10 hours), there are approximately -0.000116794382 fg/cell of *M. tuberculosis* DNA and 0.0000000000163704474 fg/cell of *M. bovis* BCG1 DNA. At the fifth time point (once more 23.10 hours), there are approximately -0.000119527363 fg/cell of *M. tuberculosis* DNA and 0.0000000000159955466 fg/cell of *M. bovis* BCG1 DNA. At the sixth time point (yet again 23.10 hours), there are approximately -0.000122324109 fg/cell of *M. tuberculosis* DNA and 0.0000000000156293192 fg/cell of *M. bovis* BCG1 DNA.

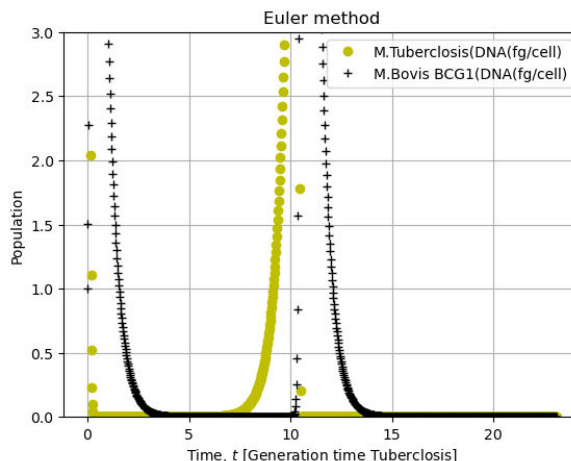


Figure: 11 Interaction of Eulers model Tuberculosis (DNA/fg/cell) and M.Bovis BCG1 (DNA/fg/cell)

Generation Time (t-days)	M.Tuberculosis(DNA(fg/cell)	M.Bovis BCG1 DNA(fg/cell)
23.10h	6.00000000e+00	1.00000000e+00
23.10h	6.02774775e+00	1.50870871e+00
23.10h	5.92799662e+00	2.28007401e+00
23.10h	1.75543657e-07	1.73882158e-10
23.10h	1.83661893e-07	1.65840764e-10
23.10h	1.92155566e-07	1.58171254e-10

Table: 11 interaction of Eulers model Tuberculosis (DNA/fg/cell) and M.Bovis BCG1 (DNA/fg/cell)

The figure 11 compares the DNA concentration (in femtograms per cell) of two types of bacteria. **Mycobacterium tuberculosis** and **Mycobacterium bovis BCG1**, over time. The time is measured in terms of the generation time of tuberculosis. The graph contains multiple curves, each representing a different initial condition (X_0) ranging from 1.0 to 6.0. Each curve shows how the DNA concentration of the two bacteria changes over time for a given initial condition. Here's a general interpretation of the graph. The x-axis represents the quantity of M. tuberculosis DNA per cell, ranging from 0 to 6. The y-axis represents the quantity of M. bovis BCG1 DNA per cell, ranging from 0 to 14. Each curve starts at the origin and extends upwards and rightwards, forming an elongated 'S' shape pattern. This suggests that as the quantity of M. tuberculosis DNA increases, the quantity of M. bovis BCG1 DNA also increases, but at a diminishing rate.

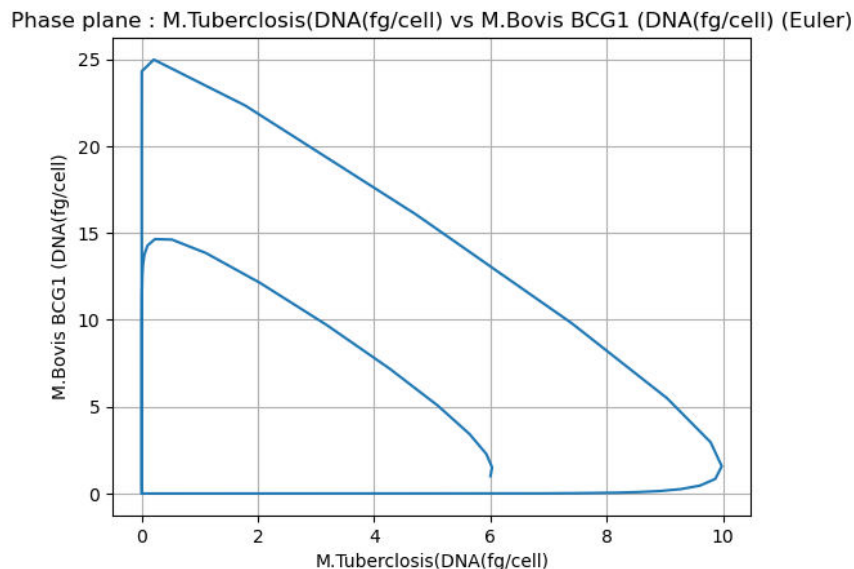


Figure: 12 Phase plane Tuberculosis (DNA/fg/cell) and M.Bovis BCG1 (DNA/fg/cell) (Euler)

The figure 12 represents a phase plane analysis comparing the DNA concentrations of *Mycobacterium tuberculosis* and *Mycobacterium bovis BCG1*, both measured in femtograms per cell (fg/cell). The x-axis corresponds to the DNA concentration of *M. tuberculosis*, while the y-axis represents the DNA concentration of *M. bovis BCG1*. The curves plotted on the graph illustrate the relationship between the

two bacterial populations over time as modelled using the Euler method. The graph shows two distinct loops, indicating different trajectories or states of interaction between the DNA concentrations of the two bacteria. Initially, *M. bovis* BCG1 DNA concentration is high when *M. tuberculosis* DNA is low. As the DNA concentration of *M. tuberculosis* increases, *M. bovis* BCG1 DNA decreases, forming a descending pattern in the graph. The first loop reaches a peak where *M. bovis* BCG1 has its maximum DNA concentration at around 25 fg/cell when *M. tuberculosis* DNA is close to 0 fg/cell. The concentration of *M. bovis* BCG1 then declines as *M. tuberculosis* DNA increases. The second loop displays a similar but slightly lower trajectory, indicating a decrease in *M. bovis* BCG1 DNA concentration as the *M. tuberculosis* concentration grows.

This phase plane suggests a competitive interaction between the two bacteria, where the presence and increase of *M. tuberculosis* DNA is associated with a decline in *M. bovis* BCG1 DNA. The loops represent the cyclic nature of this interaction, with the system returning to a lower concentration state for both bacteria as time progresses.

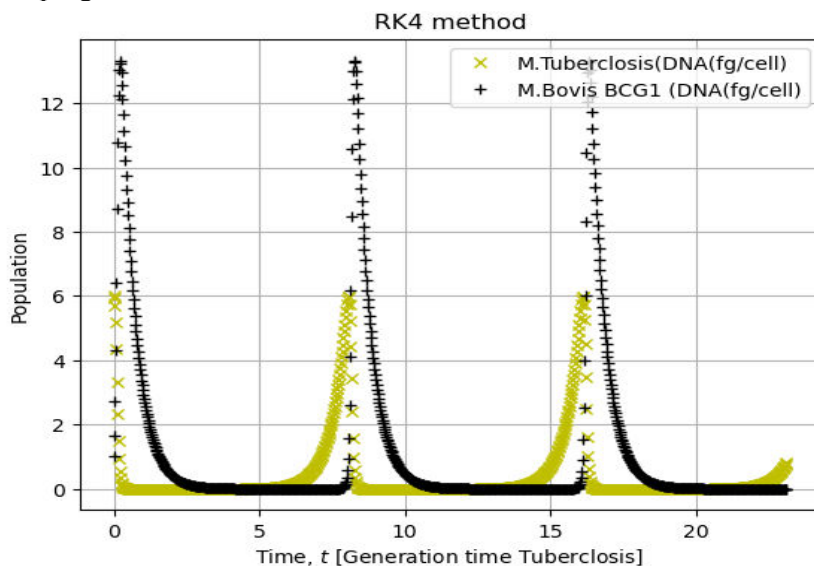


Figure: 13 Interaction of Rk4 model Tuberculosis (DNA/fg/cell) and M.Bovis BCG1 (DNA/fg/cell)

GenerationTime (t- days)	M.Tuberculosis(DNA(fg/cell))	M.Bovis BCG1 DNA(fg/cell)
23.10h	6.00000000e+00	1.00000000e+00
23.10h	5.95231967e+00	1.66128765e+00
23.10h	5.69985731e+00	2.72363306e+00
23.10h	7.38063467e-01	8.93904436e-05
23.10h	7.72994784e-01	9.15271697e-05
23.10h	8.09579264e-01	9.40253754e-05

Table: 13 Interaction of RK4 model Tuberculosis (DNA/fg/cell) and M.Bovis BCG1 (DNA/fg/cell)

The figure 13 displays the DNA concentrations of *Mycobacterium tuberculosis* and *Mycobacterium bovis* BCG1 over time, measured in femtograms per cell. The x-axis represents the DNA concentration of *M. tuberculosis*, ranging from 0 to 10 fg/cell, while the y-axis shows the DNA concentration of *M. bovis* BCG1, ranging from 0 to 25 fg/cell. The blue curve illustrates the relationship between the two bacterial DNA concentrations. As the *M. tuberculosis* DNA concentration increases, the *M. bovis* BCG1 DNA concentration initially rises steeply, but then declines after reaching its peak.

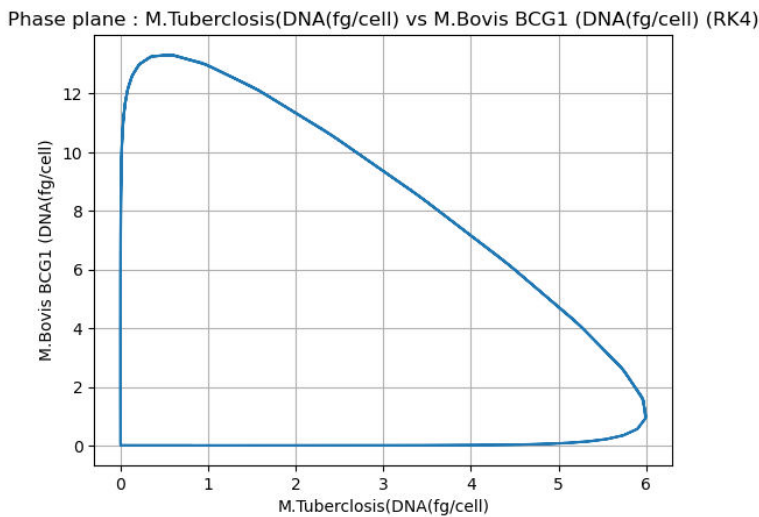


Figure: 14 Interaction of Rk4 model Tuberculosis (DNA/fg/cell) and M. Bovis BCG1 (DNA/fg/cell)

The phase plane graph compares the DNA concentrations (in femtograms per cell) of two bacterial species, *Mycobacterium tuberculosis* and *Mycobacterium bovis BCG1*. In this graph, the x-axis shows the DNA quantity of *M. tuberculosis*, ranging from 0 to 6 fg/cell, while the y-axis depicts the DNA quantity of *M. bovis BCG1*, ranging from 0 to 12 fg/cell. The blue curve illustrates the interaction between the two bacteria, indicating that as the DNA concentration of *M. tuberculosis* increases, the DNA concentration of *M. bovis BCG1* decreases significantly. This pattern suggests an inverse relationship between the two bacterial DNA concentrations.

4. Conclusion

In conclusion, this study has developed and analyzed an ordinary differential equation (ODE) model to simulate the interaction between *Mycobacterium tuberculosis* and *Mycobacterium bovis BCG1*, measured in DNA femtograms per cell. The model offers a valuable framework for understanding the dynamic relationship between these two bacterial species under various conditions. By employing both the Runge-Kutta fourth-order method and Euler's method for numerical solutions, the model demonstrates how different numerical techniques can influence the system's behavior and stability. Through the exploration of various initial conditions and parameters, the model provides insights into the complex interplay between *M. tuberculosis* and *M. bovis BCG1*. The inverse relationship observed between the DNA concentrations of these two organisms highlights the competitive dynamics inherent in their interaction. Additionally, the phase plane analysis further illustrates the stability and potential outcomes of their interactions under different scenarios. This mathematical modeling approach not only enhances our understanding of the interaction dynamics between *M. tuberculosis* and *M. bovis BCG1* but also serves as a powerful tool for researchers in the field of tuberculosis research and vaccine development. By allowing for the prediction and analysis of different scenarios, this model can contribute to the design of more effective interventions and strategies in the fight against tuberculosis and related diseases.

References

- [1]. Bansal, M., Bhattacharyya, D., and Ravi, B. (1995). NUPARM and NUCGEN: software for analysis and generation of sequence dependent nucleic acid structures. *Comput. Appl. Biosci.* 11, 281–287.
- [2]. Chiu, T. P., Comoglio, F., Zhou, T., Yang, L., Paro, R., and Rohs, R. (2016). DNAshapeR: an R/Bioconductor package for DNA shape prediction and feature encoding. *Bioinformatics* 32, 1211–1213.
- [3]. Ghoshdastidar, D., and Bansal, M. (2022). Flexibility of flanking DNA is a key determinant of transcription factor affinity for the core motif. *Biophys. J.* 121, 3987–4000.

- [4]. Gordan, R., Shen, N., Dror, I., Zhou, T., Horton, J., Rohs, R., et al. (2013). Genomic regions flanking e-box binding sites influence DNA binding specificity of bHLH transcription factors through DNA shape. *Cell Rep.* 3, 1093–1104. d
- [5]. Gunasekaran, M. and Alamelu, K. (2023). Comparative Exploration of tuberculosis in High-Risk and Low-Risk Population by Enhanced Numerical Algorithm. *Journal of Advanced Zoology*, Volume 44 Issue S8 Year 2023 Page 430441, ISSN: 0253-7214.
- [6]. Gunasekaran, M. and Alamelu, K. (2023). Enhancing Tuberculosis Modeling: The True Positive Vaccinated Approach Utilizing a Specialized Runge-Kutta Method. *Journal of Harbin Engineering University* ISSN: 1006-7043 Vol 44 No. 11.
- [7]. Gunasekaran, M. and Sarravanaprabhu, A. M. (2020). “Optimal harvesting of three species dynamics model with bionomic equilibrium”, *Turkish Journal of Computer and Mathematics Education*, Vol11. No.3, 1339-1350.
- [8]. Gunasekaran, M. and Sarravanaprabhu, A. M. (2022). “A second type of Holling functional response of stability analysis for prey predator and host ecosystem”, *Advances and Applications in Mathematical Sciences* Vol 21, Issue 11, 6213-6233.
- [9]. Gunasekaran, M. and Sarravanaprabhu, A. M. (2023). “An analysis of stability behaviour for two preys and two predators ecological model”, *Journal of Advanced Zoology* Vol 44, Issue S-8, 442-462.
- [10]. Inukai, S., Kock, K. H., and Bulyk, M. L. (2017). Transcription factor-DNA binding: beyond binding site motifs. *Curr. Opin. Genet. Dev.* 43, 110–119.
- [11]. Kumar, A., and Bansal, M. (2012). Characterization of structural and free energy properties of promoters associated with primary and operon TSS in helicobacter pylori genome and their orthologs. *J. Biosci.* 37, 423–431.
- [12]. Nature (2020). Mathematical models in the COVID-19 pandemic.
- [13]. Rohs, R., West, S. M., Sosinsky, A., Liu, P., Mann, R. S., and Honig, B. (2009). The role of DNA shape in protein-DNA recognition. *Nature* 461, 1248–1253
- [14]. Satchwell, S. C., Drew, H. R., and Travers, A. A. (1986). Sequence periodicities in chicken nucleosome core DNA. *J. Mol. Biol.* 191, 659–675.
- [15]. Sarkar, S., Dey, U., Khohliwe, T. B., Yella, V. R., and Kumar, A. (2021). Analysis of nucleoid-associated protein-binding regions reveals DNA structural features influencing genome organization in mycobacterium tuberculosis. *FEBS Lett.* 595, 2504–2521.
- [16]. Sujatha, K., and Gunasekaran, M. (2015). Two Ways of Stability Analysis of Prey-Predator System with Diseased Prey Population. *The International Journal of Engineering and Science (IIES)*, Volume-4, Issue-7, Pages 61-66, ISSN (e): 2319–1813 ISSN (p): 2319–1805.
- [17]. Sundararajan, S., Murugan, P., Jayaraman, M. S. R. (2023). Mathematical Modelling and Analysis of Tuberculosis with Vaccination Strategies. *International Journal of Mathematical Sciences and Computing*.
- [18]. The Lancet Infectious Diseases (2021). Modeling the impact of antimicrobial resistance.
- [19]. Vanaja, A., Mallick, S. P., Kulandaivelu, U., Kumar, A., and Yella, V. R. (2021). Symphony of the DNA flexibility and sequence environment orchestrates p53 binding to its responsive elements. *Gene* 803, 145892.
- [20]. Yella, V. R., Bhimsaria, D., Ghoshdastidar, D., Rodríguez-Martínez, José A., Ansari, A. Z., and Bansal, M. (2018). Flexibility and structure of flanking DNA impact transcription factor affinity for its core motif. *Nucleic Acids Res.* 46, 11883–11897.